Load optimal design for a primary test stand facility based on a zero-dimensional load model

Zhao Hai-Long(赵海龙)†, Deng Jian-Jun(邓建军),
Wang Gang-Hua(王刚华), and Zou Wen-Kang(邹文康)

Institute of Fluid Physics, China Academy of Engineering Physics, Mianyang 621900, *China*

(Received 23 July 2010; revised manuscript received 18 April 2011)

In order to couple the numerical simulation of a primary test stand driver with an optimal load design, a zero-dimensional wire array load model is designed based on the Saturn load model using PSPICE, which is an upgraded version of the Simulation Program with Integrated Circuit Emphasis (SPICE) designed by the ORCAD Corporation to perform circuit simulations. This paper calculates different load parameters and discusses factors influencing the driving current curve. With appropriate driving current curves chosen, further magneto-hydrodynamic calculations are carried out and discussed to provide the best results for experiments. The suggested optimal load parameters play an important role in experimental load design.

Keywords: Z pinch simulation, wire array load optimal design, load model

PACS: 52.65.–y, 52.65.Kj **DOI:** 10.1088/1674-1056/20/10/105201

1. Introduction

In recent years, researchers have shown that a 20-MA Z facility is capable of providing 200-TW X-ray power from a 300-tungsten wire array Z pinch load.[1−3] The wire array Z pinch appears to be the most powerful laboratory X-ray source presently available. Most Z pinch research works are carried out on real facilities by experiments, however, numerical simulations also make great contribution to Z pinch development[4−7] and calculating abilities have improved a great deal.

In parallel with activities taking place in Z facilities, since the construction of local Chinese accelerators, many Z pinch experiments and numerical simulations have been taking place on lower current machines such as the Qiang guang I generator[8−11] and the Yang accelerator.[12,13] However, a great deal of preparation is still required for the new huge Z pinch driver, the primary test stand (PTS) facility, which is still under construction at the Institute of Fluid Physics, China Academy of Engineering Physics. The main goal of the PTS facility is to obtain X-ray radiation power reaching 10 TW∼100 TW and energy transforming efficiency reaching 5%∼15% for Z pinch experiments.

In this context, the authors aim to optimize the load design for the PTS facility. In order to realize this project, first the zero-dimensional (0D) load model is introduced in Section 2, which also mentions the calculation software codes and simulation methods. In Section 3 the calculation results and analyses are listed together with the optimal load parameters. Since the Institute of Applied Physics and Computational Mathematics also has some computing results about the PTS load design,[14] in Section 4 we give a comparison with their results. Finally, a conclusion is provided.

2. Load model and simulation codes

Every driver facility has its corresponding simulation codes available long before its construction, such as the SCREAMER[15] and TL[16] codes, both of these codes were used to design the Z pinch modification for the Z facility; and the ZORK code, which is a modified circuit code designed for the Saturn facility to make implosion simulations of Z pinch. In conjunction with the full circuit and equivalent circuit simulation methods, all of these codes are designed for the simulation of a working facility and its examination, providing numerical results for subsequent experiments from a computational point of view.

†Corresponding author. E-mail: dragonfly1985@gmail.com

© 2011 Chinese Physical Society and IOP Publishing Ltd

Following this method, the authors are attempting to create a corresponding simulation platform, including numerical codes and the full circuit simulating method for the PTS before it is fully built. This platform consists of three main parts: the 0D load model using PSPICE; the full circuit simulation using PSPICE; and the radiation magneto-hydrodynamic code MHD1. These three parts together will become a whole computing system for the PTS, which is capable of evaluating the facility working under different conditions. In addition, the load implosion time, the radius and time traces, and radiation X-ray power and energy could also be obtained by this system.

2.1. Zero-dimensional load model

The ZORK[17] code is a 0D load model program designed by the Sandia Laboratory for the Saturn facility. Its core idea is the dynamic load inductance used for calculations, which is also the most popular simulation method used by usual computing projects. Its equivalent circuit is shown in Fig. 1.

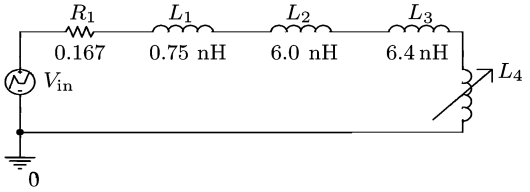


Fig. 1. Equivalent circuit simulation of the ZORK code for Saturn.

In Fig. 1 the $V_{\rm in}$ represents the voltage coming from the transmission line, usually taking the values measured from experiments; R_1 and L_1 are the resistance and inductance of the transmission line, respectively; L_2 and L_3 are constant inductances relating to the load initiation. All of the above are used with the international system of units (SI units). The dynamic model of the wire array load and the corresponding load dynamic inductance are described by Eqs. (1) and (2), respectively

$$m\frac{{\rm d}v}{{\rm d}t} = 2\pi Rl\frac{B^2}{2\mu_0}, \tag{1}$$

$$L_4(t) = \frac{\mu_0 l(N-1)}{2\pi N}\ln\left(\frac{R_i}{R(t)}\right). \tag{2}$$

In these equations, $\mu_0 = 4\pi \times 10^{-7}$ H/m, $B = \mu_0 I/2\pi R$, $R(t) = R(0) - \int_{t_i}^{t} v(t')\,{\rm d}t'$, $v(t) = \int_{t_i}^{t} (l/m)\cdot(\mu_0 I^2)/(4\pi R(t'))\,{\rm d}t'$, $R_{\rm i}$ is the wire array initial radius, N is the wire number and l is the length of the wire load. All parameters in Eqs. (1) and (2) are used with SI units.

2.2. Full circuit model and MHD1 code

The PSPICE is used to translate the ZORK load model into computer code. Considering the interactive influences between the implosion load and the driver facility circuit, the full circuit model must be adopted. This is also the most important difference between our computing and others, as usually the equivalent circuit is used to make simulations simple, and this equivalent circuit cannot reveal the connections between load implosion and the driving facility circuit. PSPICE is used to simulate the driving facility circuit and the 0D load model is mounted with it, forming a whole implosion circuit from which the load driving current can be obtained. Further radiation calculation can be made using the acquired current curve. However, the optimal choice should be decided first to make sure that the obtained current curve is appropriate for experimental load design.

As a 0D mode, ZORK cannot deal with the implosion radiation calculation, so, with the appropriate current curve acquired, further radiation simulations will require the MHD1 code. The MHD1 is a one-dimensional (1D) magneto-hydrodynamic numerical simulation code designed for Z pinch implosion; it belongs to department 105 in the Institute of Fluid Physics and can provide key implosion parameters such as the implosion time, implosion velocity, radiation power, energy, etc. Given the current curve acquired from the PTS PSPICE simulation, results can be obtained from MHD1 with different initializations and the further load optimal design can be made by this.

3. Simulation results and discussion

To search for the optimal load design, the relations between driving current and load initialization must be understood first. To achieve this, the Saturn classical load parameters[17] are used to calculate for a first view of the PTS driving ability. The load radius R is chosen to be 2 mm, load length to be 2 cm and load mass to be 4.7 mg, the load material is chosen to be tungsten. The acquired driving current is shown in Fig. 2(a), whose maximum current level is about 9.6 MA and the current rising time (10%$I_{\rm max}$ ~90% $I_{\rm max}$) is about 90 ns.

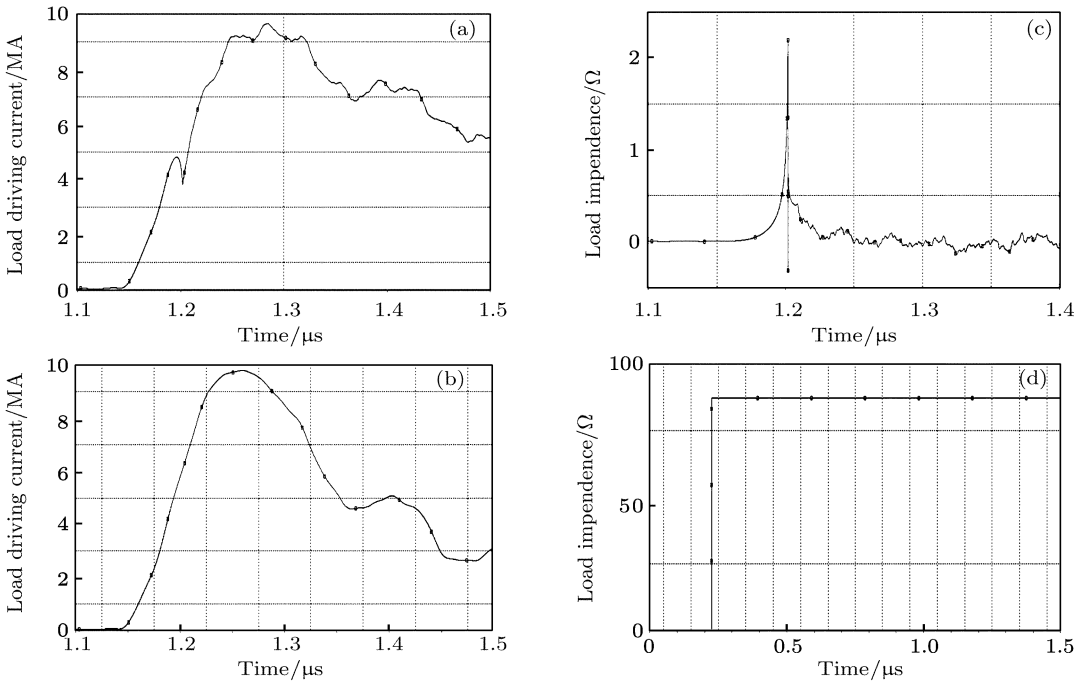


Fig. 2. Load driving current and impedance change curve, in which panels (a) and (b) correspond to driving current of the 0-D load and constant value load, respectively; panels (c) and (d) correspond to their impedance change curve, respectively.

However, the current curve is strongly anomalous and at some times has a strong jump. This is probably caused by the strongly anomalous impedance change during implosions. To check this out, a constant resistance load is used to obtain the corresponding current curve. The resistance of the load is calculated with a load radius of 2 mm, a load length of 2 cm and a load mass of 4.7 mg. The constant load resistance is calculated to be 0.0873 Ω. Plots of the calculation results with constant load and changeable impedance load together are shown in Figs. 2(b), 2(c), and 2(d). Figure 2(b) shows the driving current when the load is a constant value resistance, figures 2(c) and 2(d) show the impedance change for the two different loads, respectively.

According to Fig. 2, the anomalous driving current curve coincides with the corresponding impedance change and the strong jump of the current corresponds to the maximum impedance during the implosion time. Take the 0D load as an example. When the time comes to about 1.20 μs, the impedance reaches its maximum value and the corresponding current curve also has a big jump. Considering the dynamic inductance function (2), we can reveal that this time is also the time when the wire load stagnates on the load axis.

To check this out, the load radius trace is plotted in Fig. 3, in which the voltage of LIMIT:Out represents the wire array radius change during our calculation model. From Fig. 3, the implosion time is also found to be about 1.20 μs. So the time when the load radius comes to the load axis and the time when the load maximum inductance arrives are identical, the same is true for the corresponding current curve jump time.

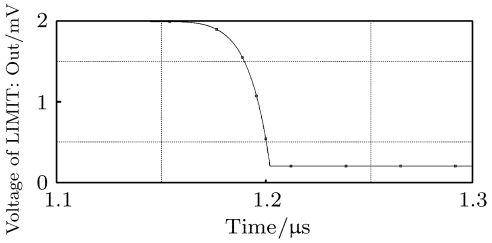


Fig. 3. Radius–time plot curve of the Saturn zero-dimensional load model.

These calculation results explain the anomaly and jump of the driving current curve, showing a first view of the PTS driver and the same value of three important times also proves the ZORK load model to be correct. However, to create an optimal load design, further studies about the relations between driving current and load initialization, such as load radius R and load mass m, are going to be performed.

3.1. Driving current versus load radius

By summarizing the classical experimental data of huge drivers such as Saturn and the Z facility, it could be found that the load length was usually fixed

and unchangeable, and the changeable parameters are usually load radius and load mass. The load length is usually set to be 2 cm in experiments, so in the following calculations, the load length is also set unchangeably to be 2 cm. The relations between driving current and load initialization such as load radius and load mass are mainly discussed.

The load length was kept at 2 cm and the values of load mass were set to be 4.7 mg, 4.0 mg, and 2.5 mg, respectively, while the load radius is changeable, calculations are preformed and the results are obtained; the results we are concern with such as the maximum current and time, the implosion time and current, and the time difference between the two key times are listed in Table 1.

From the calculated results listed in Table 1, it is found that while the load length (denoted by l) and load mass (denoted by m) are fixed, as the load radius increases, the implosion time is getting later, and this coincides with experimental directions; it is also found that for some given load mass, there exists a threshold R_x for the load radius (R_x is about 7 mm when the load mass is fixed at 4.7 mg). When the radius is larger than this R_x, the implosion time is later than the maximum current time ($\mathrm{d}t > 0$), or else the implosion time is earlier than the maximum current time. To make the best use of driver energy, it is required that the implosion time is close to the maximum current time, or slightly later than it. Following this guide, the load parameters chosen for the MHD1 calculation should be decided by the value of time difference $\mathrm{d}t$. For all parameters in Table 1, only the parameters corresponding to $\mathrm{d}t = 16.3$ ns and 17.4 ns are suitable. However, to make final decision of the initialization for MHD1 calculation, further research about the relationship between driving current and load mass is needed.

Table 1. Calculated results of different load radii for a fixed load mass.

Load initialization (R/m, m/kg, l/m)	Maximum current and time (t/μs, I/MA)	Implosion time and current (t/μs, I/MA)	Time difference ($\mathrm{d}t_{\mathrm{imp}}$–$\mathrm{d}t_{I\,\mathrm{max}}$) $\mathrm{d}t$/ns
$R = 2.0 \times 10^{-3}$, $m = 4.7 \times 10^{-6}$, $l = 2 \times 10^{-2}$	$t = 1.2844$, $I = 9.670$	$t = 1.2019$, $I = 3.8323$	−82.5
$R = 8.8 \times 10^{-3}$, $m = 4.7 \times 10^{-6}$, $l = 2 \times 10^{-2}$	$t = 1.2345$, $I = 9.785$	$t = 1.2519$, $I = 7.4451$	17.4
$R = 1.0 \times 10^{-2}$, $m = 4.7 \times 10^{-6}$, $l = 2 \times 10^{-2}$	$t = 1.2389$, $I = 10.117$	$t = 1.2587$, $I = 7.6647$	19.8
$R = 8.8 \times 10^{-3}$, $m = 4.0 \times 10^{-6}$, $l = 2 \times 10^{-2}$	$t = 1.2316$, $I = 9.570$	$t = 1.2479$, $I = 7.3054$	16.3
$R = 1.0 \times 10^{-2}$, $m = 4.0 \times 10^{-6}$, $l = 2 \times 10^{-2}$	$t = 1.2362$, $I = 9.910$	$t = 1.2546$, $I = 7.5930$	18.4
$R = 1.0 \times 10^{-2}$, $m = 2.5 \times 10^{-6}$, $l = 2 \times 10^{-2}$	$t = 1.2888$, $I = 9.638$	$t = 1.2431$, $I = 7.1048$	−45.7
$R = 3.0 \times 10^{-2}$, $m = 2.5 \times 10^{-6}$, $l = 2 \times 10^{-2}$	$t = 1.2613$, $I = 11.491$	$t = 1.3229$, $I = 7.1691$	61.6

3.2. Driving current versus load mass

Still keeping the load length at 2 cm, this time we fix the load radii at 8.8 mm, 10 mm, and 30 mm respectively, while the load mass is changeable. Our attention is still attracted by key parameters like the maximum current and time, the implosion time and current, and the time difference between the two key times, etc. Calculations of these parameters are performed and the results are listed in Table 2.

From the calculated results listed in Table 2, it is found that while the load length and load radius are fixed, as the load mass grows heavier, the implosion time beomes later and later, and this can be seen more clearly in Fig. 4(a). Just like the former calculations in which the load mass is fixed, this time it is also found that for a given load radius, there exists a threshold m_x for the load mass (m_x is about 3.5 mg for a load radius fixed at 8.8 mm). When the load mass is heavier than this m_x, the implosion time is later than the maximum current time ($\mathrm{d}t > 0$), or else the implosion time is earlier than the maximum current time. This can be seen more clearly in Fig. 4(b) and from that figure it is also found that before this threshold m_x the gradient of the time difference curve is very large while after this threshold, the curve becomes smooth.

Still following the guide of making best use of driver energy, for the parameters listed in Table 2, the parameters corresponding to $\mathrm{d}t = 16.3$ ns and 18.4 ns are suitable for MHD1 calculation; combine this with the former chosen parameters for $\mathrm{d}t = 16.3$ ns and 17.4 ns, it could be concluded that the parameters for $\mathrm{d}t = 16.3$ ns are the best ones suitable for the MHD1 radiation calculation. It also means that the load initialization chosen for MHD1 calculation are set to be load radius $R = 8.8$ mm, load mass $m = 4.0$ mg, and load length $l = 2$ cm.

Table 2. Calculated results of different load masses for fixed load radius.

Load initialization (R/m, m/kg, l/m)	Maximum current and time (t/μs, I/MA)	Implosion time and current (t/μs, I/MA)	Time difference (dt_{imp}–$dt_{I\,max}$)dt/ns
$R = 8.8 \times 10^{-3}$, $m = 4.7 \times 10^{-6}$, $l = 2 \times 10^{-2}$	$t = 1.2345$, $I = 9.785$	$t = 1.2519$, $I = 7.4451$	17.4
$R = 8.8 \times 10^{-3}$, $m = 4.5 \times 10^{-6}$, $l = 2 \times 10^{-2}$	$t = 1.2337$, $I = 9.727$	$t = 1.2508$, $I = 7.4052$	17.1
$R = 8.8 \times 10^{-3}$, $m = 4.0 \times 10^{-6}$, $l = 2 \times 10^{-2}$	$t = 1.2316$, $I = 9.570$	$t = 1.2479$, $I = 7.3054$	16.3
$R = 8.8 \times 10^{-3}$, $m = 2.1 \times 10^{-6}$, $l = 2 \times 10^{-2}$	$t = 1.2801$, $I = 9.795$	$t = 1.2340$, $I = 6.6667$	–46.1
$R = 1.0 \times 10^{-2}$, $m = 5.0 \times 10^{-6}$, $l = 2 \times 10^{-2}$	$t = 1.2399$, $I = 10.193$	$t = 1.2605$, $I = 7.7365$	20.6
$R = 1.0 \times 10^{-2}$, $m = 4.7 \times 10^{-6}$, $l = 2 \times 10^{-2}$	$t = 1.2389$, $I = 10.117$	$t = 1.2587$, $I = 7.6647$	19.8
$R = 1.0 \times 10^{-2}$, $m = 4.0 \times 10^{-6}$, $l = 2 \times 10^{-2}$	$t = 1.2362$, $I = 9.910$	$t = 1.2546$, $I = 7.5930$	18.4
$R = 1.0 \times 10^{-2}$, $m = 2.5 \times 10^{-6}$, $l = 2 \times 10^{-2}$	$t = 1.2888$, $I = 9.638$	$t = 1.2431$, $I = 7.1048$	−45.7
$R = 3.0 \times 10^{-2}$, $m = 5.5 \times 10^{-6}$, $l = 2 \times 10^{-2}$	$t = 1.2645$, $I = 11.749$	$t = 1.3858$, $I = 5.7239$	121.3
$R = 3.0 \times 10^{-2}$, $m = 2.5 \times 10^{-6}$, $l = 2 \times 10^{-2}$	$t = 1.2613$, $I = 11.491$	$t = 1.3229$, $I = 7.1691$	61.6
$R = 3.0 \times 10^{-2}$, $m = 1.5 \times 10^{-6}$, $l = 2 \times 10^{-2}$	$t = 1.2583$, $I = 11.159$	$t = 1.2963$, $I = 7.8094$	38
$R = 3.0 \times 10^{-2}$, $m = 0.5 \times 10^{-6}$, $l = 2 \times 10^{-2}$	$t = 1.2382$, $I = 10.062$	$t = 1.2573$, $I = 7.7332$	19.1

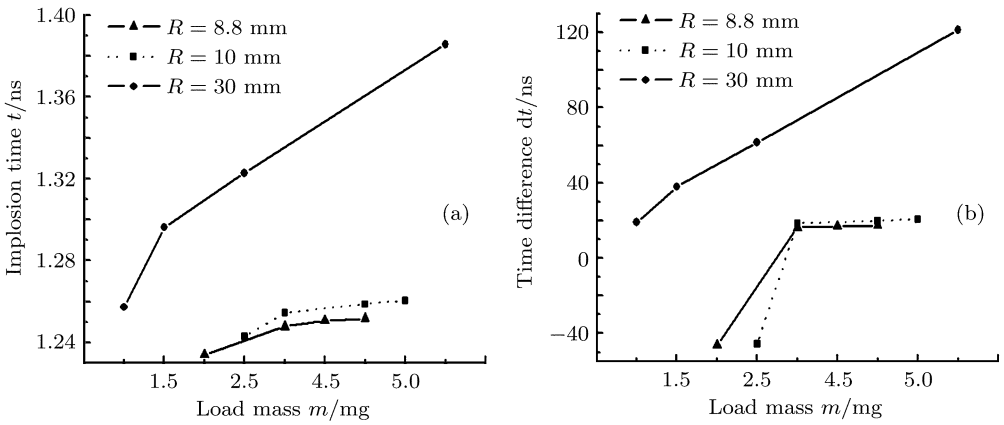


Fig. 4. Calculated results of different load masses for a fixed load radius: (a) implosion time versus load mass and (b) time difference versus load mass.

3.3. Optimal load parameters for experiment

The MHD1 is a 1D magneto-hydrodynamic code designed for Z pinch numerical simulations. It has been applied to many models and the results have been proven to be correct, so in this article the authors use this code for further radiation calculations. The parameters used for calculation are set to be load radius $R = 8.8$ mm, load mass $m = 4.0$ mg, and load length $l = 2$ cm, and the driving current simulation with PSPICE is shown in Fig. 5.

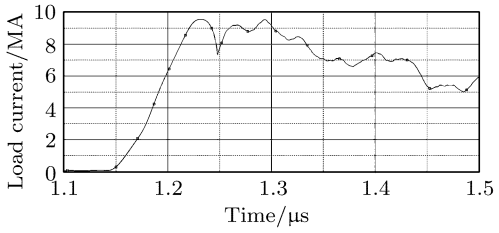


Fig. 5. Driving current curve of parameter $R = 8.8$ mm, $m = 4.0$ mg, $l = 2$ cm.

From Fig. 5 it is found that the implosion time is about 108 ns, later than the maximum current time. Taking the driving current curve as the current input for MHD1, the calculation parameters are set to be $R = 8.8$ mm, $m = 4.0$ mg, and $l = 2$ cm, and the load material is chosen to be tungsten. The simulation can then be performed and the numerical results obtained. From the results it is found that the implosion time is also 108 ns, which coincides with the PSPICE calculating results and for obtaining the radiation effect of Z pinch, the radiation power is plotted and shown in Fig. 6.

It is found in Fig. 6 that the calculated radiation power is about 70 TW, almost the best result of Saturn experimental data (∼75 TW); this result also proves that the parameters chosen for calculation are correct and reveals the basic driving ability of the PTS facility, which provides more information about the driver.

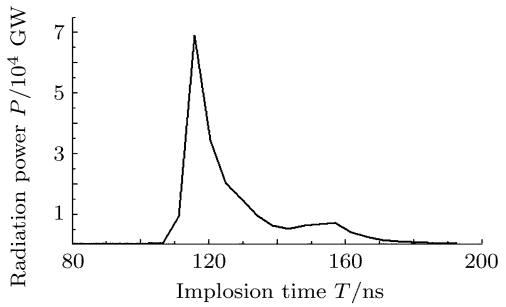


Fig. 6. Radiation power of parameter $R = 8.8$ mm, $m = 4.0$ mg, $l = 2$ cm.

However, the parameters chosen for calculation just prove that the energy is theoretically put to its best use, but the radiation power may not be at its highest, more calculations should be made to find the best output power. So the closest (from $\mathrm{d}t = 16.3$ ns) $\mathrm{d}t = 17.4$ ns and 18.4 ns parameters are chosen to make further calculations for comparison. Tungsten is still chosen for use as the load material and the load parameters are set, respectively, to be a) $R = 8.8$ mm, $m = 4.7$ mg, $l = 2$ cm; b) $R = 10$ mm, $m = 4.0$ mg, $l = 2$ cm. Calculations of the two parameters are then carried out and the radiation powers are shown in Fig. 7.

From Fig. 7(a) it is found that the radiation curve is almost the same as shown in Fig. 6. The power is still about 70 TW, the only difference between them is a few nanoseconds delay of the implosion time. However, in Fig. 7(b) the output radiation power (100 TW) of parameters $R = 10$ mm, $m = 4.0$ mg, $l = 2$ cm is obviously higher than that of parameters $R = 8.8$ mm, $m = 4.0$ mg, $l = 2$ cm. Therefore, the parameters suggested for experiments should be the load radius $R = 8.8$ mm, load mass $m = 4.0$ mg, and load length $l = 2$ cm.

In order to provide an accurate initialization for experimental load, the load wire number should be considered. According to Haines' heuristic model,[18] the critical wire number is given out by $n_{\mathrm{c}} = \pi r_0/vt_{\mathrm{p}}$, while the implosion velocity is given as 5 km/s, the implosion time as 100 ns and load radius as 1 cm; then the critical number could be obtained to be $N_{\mathrm{c}} = 62.8$. So if the single wire radius chosen to be 5 μm (the most useful size taken in experiments), the load wire number is obtained to be $132 > 62.8$, which fulfills the demand of critical number and is suitable for experimental load initialization.

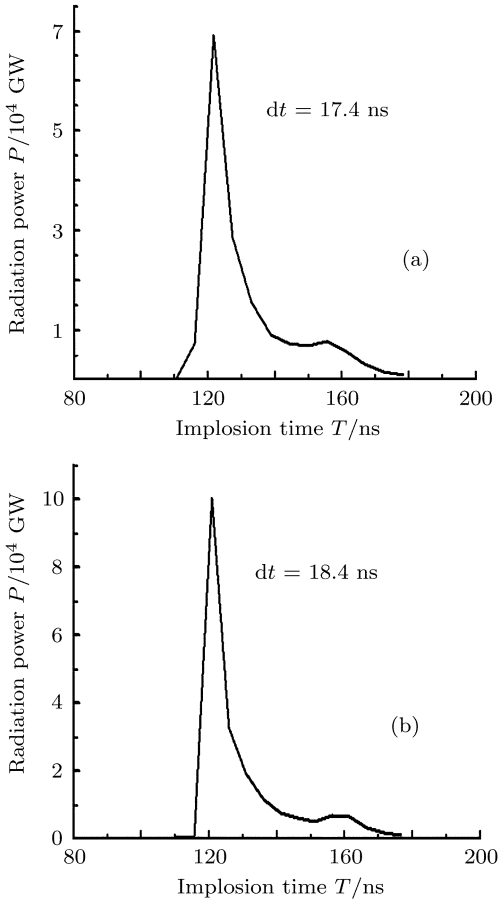


Fig. 7. Radiation power of $\mathrm{d}t = 17.4$ ns and 18.4 ns parameters: (a) $R = 8.8$ mm, $m = 4.7$ mg, $l = 2$ cm; (b) $R = 10$ mm, $m = 4.0$ mg, $l = 2$ cm.

4. Conclusion and comparison

The 0D load model is combined with the PTS driver facility using PSPICE; calculations of different initial parameters are made; the relationships between driving current and load radius and load mass are found. Following the guide of making best use of driver energy, optimal parameters are chosen for MHD1 calculations. Using the driving current obtained from PSPICE for the MHD1 current input, the chosen optimal parameters are set to make numerical simulations and results obtained and compared, finally the best initial load parameters suggested for experiment are given.

After a series of calculations and discussions, the optimal load design for the PTS facility could be concluded as the following: the driving current of PTS is about 10 MA and rising time of current is about 90 ns ($10\%I_{\max}$~$90\%I_{\max}$); the optimal load parameter range should be load radius R evaluated between 8.75 mm~10 mm, load mass evaluated between

4 mg∼5 mg and load length set to be 2 cm constant; the estimated implosion time is about 120 ns, the output radiation power is about 70 TW∼100 TW, radiation energy is about 700 kJ and the energy transforming efficiency is around 10%. Generally speaking, the driving ability of the PTS is at the same level as Saturn, but it is slightly better than it, depending on the load optimal design.

The Institute of Applied Physics and Computational Mathematics also has some computing results about the PTS load design. Compared with them, our optimal results are more accurate because of the full circuit model. Their results focus on the analysis of driving ability and the load parameter range is wide, while our calculations focus more on the optimal load design and the parameter range is shorter than theirs. Finally the most important difference, the best optimal load parameters for experiment, are given out accurately in our calculations: load wire number N is 132 while single wire radius is 5 μm, and load material is chosen to be tungsten; the load radius and mass is set to be 10 mm and 4.0 mg, respectively, while the load length is kept constant 2 cm; the estimated implosion time is about 120 ns, the radiation power is around 100 TW, the radiation energy is about 1 MJ and the energy transforming efficiency is around 15%, this is almost the best driving ability of the PTS facility.

The results of our calculation provide good advance information about the PTS facility, and play an important role in load optimal design. However, due to a lack of time and personal ability, there are also some shortcomings, such as we do not discuss the influences on driving current while the load length and compression ratio are changeable, this is going to be our further research.

References

[1] Deeney C, Douglas M R, Spielman R B, Nash T J, Peterson D L, L'Eplattenier P, Chandler G A, Seamen J F and Struve K W 1997 *Phys. Rev. Lett.* **81** 4883

[2] Spielman R B, Deeney C, Chandler G A, Douglas M R, Fehl D L, Matzen M K, McDaniel D H, Nash T J, Porter J L, Sanford T W L, Seaman J F, Stygar W A, Struve K W, Breeze S P, McGurn J S, Torres J A, Zagar D M, Gilliland T L, Jobe D O, Mckenney J L, Mock R C, Vargas M, Wagoner T and Peterson D L 1998 *Phys. Plasmas* **5** 2105

[3] Cuneo M E, Waisman E M, Lebedev S V, Chittenden J P, Stygar W A, Chandler G A, Vesey R A, Yu E P, Nash T J, Bliss D E, Sarkisov G S, Wagoner T C, Bennett G R, Sinars D B, Porter J L, Simpson W W, Ruggles L E, Wenger D F, Garasi C J, Oliver B V, Aragon R A, Fowler W E, Hettrick M C, Idzorek G C, Johnson D, Keller K, Lazier S E, McGurn J S, Mehlhorn T A, Moore T, Nielsen D S, Pyle J, Speas S, Struve K W and Torres J A 2005 *Phys. Rev.* E **71** 046406

[4] Katzenstein J 1981 *J. Appl. Phys.* **52** 676

[5] Velikovich A L, Davis J, Thornhill J W, Giuliani J L, Rudakov L I and Deeney C 2000 *Phys. Plasmas* **7** 3265

[6] Xiao D L, Ning C, Lan K and Ding N 2009 *Acta Phys. Sin.* **58** 430 (in Chinese)

[7] Huang J, Sun S K, Xiao D L, Ding N, Ning C, Zhang Y and Xue C 2010 *Acta Phys. Sin.* **59** 6351 (in Chinese)

[8] Wang L P, Qiu A C, Kuai B, Cong P T, Liang T X, Zhang Z, Jia W and Guo N 2004 *High Power Laser and Particle Beams* **16** 261 (in Chinese)

[9] Ning C, Ding N and Yang Z H 2007 *Acta Phys. Sin.* **56** 338 (in Chinese)

[10] Qiu A C, Kuai B, Wang L P, Wu G and Cong P T 2008 *High Power Laser and Particle Beams* **20** 1911 (in Chinese)

[11] Wu G, Qiu A C, Lü M, Kuai B, Wang L P, Cong P T, Qiu M T, Lei T S, Sun T P, Guo N, Han J J, Zhang X J, Huang T, Zhang G W and Qiao K L 2009 *Acta Phys. Sin.* **58** 4779 (in Chinese)

[12] Xie W P, Wang W D, Deng J J, Ying C T and Ding B N 2003 *High Power Laser and Particle Beams* **15** 25 (in Chinese)

[13] Huang X B, Lin L B, Yang L B, Deng J J, Gu Y C, Ye S C, Yue Z P, Zhou S T, Li F P and Zhang S Q 2005 *High Power Laser and Particle Beams* **17** 793 (in Chinese)

[14] Ding N, Zhang Y, Ning C, Shu X J and Xiao D L 2008 *Acta Phys. Sin.* **57** 3027 (in Chinese)

[15] Struve K W, Martin T H, Spielman R B, Stygar W A, Corcoran P A and Douglas J W 1997 *IEEE Conference Record: Abstracts* (IEEE Pulsed Power and Plasma Conference), 1997, 29 June–2 July, Baltimore, USA p. 162

[16] Corcoran P A, Douglas J W, Smith I D, Spence P W, Stygar W A, Struve K W, Martin T H, Spielman R B and Ives H C 1997 *IEEE Conference Record: Abstracts* (IEEE Pulsed Power and Plasma Conference), 1997, 29 June–2 July, Baltimore, USA p. 466

[17] Sanford T W L, Humphreys D R, Poukey J W, Marder B M, Halbleib J A, Crow J T, Spielman R B and Mock R C 1994 *Sandia National Laboratories Report* **SAND8921315**

[18] Haines M G 1998 *IEEE Trans. Plasma Sci.* **26** 1275